Bangl. J. Vet. Med. (2023). 21 (1): 7–15 ISSN: 1729-7893 (Print), 2308-0922 (Online)

Received: 10-02-2023; Accepted: 15-05-2023 DOI: https://doi.org/10.33109/bjvmjj2023zm1

ORIGINAL ARTICLE

Morphometric analysis of adult Hippopotamus forelimb bones

M. J. H. Shuvo, R. I. Shuvo, A. A. Emran, M. T. Rahman, I. H. Robin, M. K. Hasan, M. A. Jahid, M. T. Hussan, M. S. Rahman*

Department of Anatomy and Histology, Faculty of Animal Science and Veterinary Medicine, Patuakhali Science and Technology University, Bangladesh.

Email of authors: M.J.H.S. (jafrulshuvo15@gmail.com); R.I.S. (rejaulislam537@gmail.com); A.A.E. (emran.dvm15.pstu@gmail.com); M.T.R. (tareqpstu18@gmail.com); I.H.R. (Istiakrobin3@gmail.com); M.K.H (khaliddvmpstu@gmail.com); M.A.J. (majahid@pstu.ac.bd); M.T.H. (tufazzal84@gmail.com); M.S.R. (saidur@pstu.ac.bd)

Abstract

Background: Understanding the adaptative changes in bone shapes among animals involves studying bone morphology. We examined adult hippopotamus (Hippopotamus amphibius)forelimb bones at the anatomy laboratory of Patuakhali Science and Technology University, Bangladesh. Samples were collected from Rangpur Recreation Park and Zoo between September 2021 and July 2022.

Methods: Bones were processed by removing mud and boiled with water. Subsequently, hydrogen peroxide was used for one and a half hours to remove any remaining muscular tissues from the bones. Following this, the bones were air-dried under sunlight for a month. Measurements of key parameters including length, height, width, circumference, and weight were obtained using calibrated instruments, thereby ensuring precision.

Results: The scapula displayed a pronounced and elongated spine – the spina scapulae – that demarcated the lateral surface into two distinct fossae: the supraspinous fossa and the infraspinous fossa. The distal expansion of the spine, known as the acromion process, consisted of the fused hamate process and suprahamate process. The head of humerus was round and featured two undivided tubercles: the greater or major and the lesser tubercle. On the medial surface, a small and shallow radial fossa was observed, while on the opposite side, a large and deep olecranon fossa was present. The proximal surface of the radius head exhibited concave fovea capitis radii, which articulated with the lateral condyle of the humerus. The shaft of the radius was slightly expanded in the cranio-caudal direction. Similarly, the shaft of the ulnahad a somewhat triangular shape, resembling the shape of the radius shaft. Medially, it had a convex facet that articulated with the radius, and cranially, the interosseous space between the radius and ulna was longer than the caudal view.

Conclusions: The unique anatomical features and morphometric measurements of the forelimb bones in hippos can be beneficial for identification, radiographic interpretation, and forensic investigation. Furthermore, this study provides essential guidelines and insights for understanding appropriate anatomical parameters.

Key words: Hippopotamus, anatomy, scapula, humerus, radius, ulna

*Correspondence: saidur@pstu.ac.bd

Introduction

Osteology plays a crucial role in taxonomic identification and classification. The hippopotamus, often referred to as the 'hippo', is the largest semi aquatic mammal native to sub-Saharan Africa. It belongs to the family Hippopotamidae and comprisestwo extant species, the common hippopotamus and the pygmy hippopotamus. The name 'hippopotamus' is derived from the ancient Greek words meaning 'river horse'. Unlike other aquatic mammals, the hippopotamus is seldom found entirely submerged, as it prefers to maintain contact with the river or lake bottoms. Instead of swimming, it moves by walking underwater. This behavior is facilitated by the management of its body's specific gravity and the presence of high bone density (Eltringham, 1999; Feldhamer *et al*., 1999; Fisher *et al*., 2007; Klingel, 1991; Nowak, 1999; Wall, 1983).

Research has investigated the hippo's skeletal structure, revealing its adaptation as a graviportal animal capable of supporting its immense weight. This specialized structure not only aids in weight-bearing but also facilitates the ability of hippos to move along the bottom of water bodies (Brittany and Frank, 2009). The hippopotamus possesses well-developed musculature, particularly in the chest and forelimbs, which contributes to its robust physique. To accommodate and sustain these powerful muscles akin to architectural columns, the hippo's shoulder, elbow, and radiocarpal joints are vertically aligned, with the scapula positioned downward in harmony with the overall bone architecture (Nzalak *et al*., 2010). While extensive studies have examined the skeletal systems of large animals such as horses, cattle, small ruminants like sheep and goats (Sisson *et al*., 1975), and wild carnivores like tigers (Tomar *et al*., 2018) limited literature exists concerning systematic information on distinctive anatomical features of hippo bones. Osteomorphometrical features hold significant value, particularly in the field of radiology and forensic studies. Despite their importance, a detailed morphometrical analysis of the hippo's skeletal system has yet to be undertaken. Given this gap in understanding, the present study was undertaken to address this very matter.

Materials and Methods

Study area and period

The research took place within the Anatomy laboratory of Patuakhali Science and Technology University, located in Bangladesh. The study focused on examining the scapula, humerus, radius, and ulna of a fully grown hippopotamus. This specific hippopotamus had suddenly died at Recreation Park and Rangpur Zoo in Rangpur on 27 February 2021. As part of proper procedures, the animal was buried in designated isolated areas within the zoo's burial ground, following aseptic measures.

Carcass processing for bone specimens

The hippopotamus was over 37 years old at the time of death. The carcass was buried underground for six months immediately following its death. In September 2021, after this incubation period, the bones were retrieved and subjected to meticulous preparation. After six months the bones were collected and subjected to thorough processing. Initially, the bones were cleansed to eliminate adhering mud and debris. Subsequently, boiling in water facilitated the removal of residual soft tissue. A hydrogen peroxide (H2O2) treatment lasting one and a half hours was then employed to ensure complete elimination of any remaining muscular components from the bones. Following the complete removal of muscular structures using knives and surgical blades, a thorough rinse with clean water was conducted for all bones. Subsequently, the bones were carefully air-dried under sunlight for a month. This rigorous processing protocol ensured optimal preparation of the bones for subsequent examination and analysis.

Morphometric analysis

A comprehensive morphometric analysis was conducted utilizing a precisely calibrated scale. Measurements of length, height, width, and circumference were taken and documented in centimeters (cm). Additionally, weight was determined with the aid of a digital balance and recorded in grams (g). All the data were analyzed by using Graphpad prism 5 software.

Results and Discussion

Scapula

Anatomically, the scapula (plural scapulae or scapulas), commonly referred to as the shoulder bone, shoulder blade, side bone, speal bone, or blade bone connects the humerus (upper arm bone). In the hippopotamus, this scapula takes on a distinctive downward and forward-oriented triangular shape, positioning itself within the cranio-lateral region of the chest. Notably, its dorsal end is comparatively broader, while the ventral end is narrower. In contrast, the scapula in other animals such as tigers (Tomar *et al*., 2018), Indian wild cats (Palanisamy *et al*., 2018) and civet cats (Sarma *et al*., 2017) assumes a quadrangular shape. In the case of the hippopotamus, the slightly sloped scapula plays a pivotal role in accommodating the lateral configuration of the forelimb. The morphometrical data for different parameters of the hippopotamus scapula are presented in Table 1.

The scapula is composed of two upper parts, three margins, and three peripheries. The lateral surface is divided by a well-developed elongated flat known as the 'spina scapulae', which separates it into two distinct fossae: the supraspinous fossa (fossa supraspinata) and the infraspinous fossa (fossa infraspinata) (Fig. 1). However, similar paired fossaeare observed in the dog (Miller *et al*., 2008; Sisson *et al*., 1975) and the Indian wild cat (Palanisamy *et al*., 2018). The height of the scapular middle line spine gradationally diminishes and fuses toward the proximal limb. The spine's border extends towardthe infraspinous fossa, except forits distal one-fourth part. In contrast, the proximal one-third is slightly rugged and thickened, similar findings reported in tiger (Tomar *et al*., 2018). The distal expansion of the spine, namely the acromion process, comprises the hamate process (*processus hamatus*) and the suprahamate process (*processus suprahamatus*), which are fused together (Fig. 1a).

The hamate process displayed a triangular shape with thick blunt prominent ends that were sealed by the glenoid depression (*cavitas glenoidalis*), appearing a rough tip. At the tip's end, a slightly flattened spine pointed backward (Fig. 1a). This flat configuration was consistent with findings in cattle, sheep, and goats (Sisson *et al*., 1975). The suprahamate process resembled a thick triangular plate, fused with the hamate process (*processus suprahamatus*). Similarly, the supraglenoid excrescence (*tuberculum supraglenoidalis*) was present in hippos, like observations in horses (Sisson *et al*., 1975) and cattle (Budras and Habel, 2011). The surface of the supraspinous fossa featured a centrally deep, undulating, concavity that dorsally transitioned into convexity and showed an incipient concave curvature towards the spine. The infraspinous fossa displayed nearly analogous traits but with less pronounced undulation and a flatter aspect on the side (Fig. 1a). This result shared similarity with that of lion (Nzalak *et al*., 2010) but was partially comparable to findings in tigers (Tomar *et al*., 2018) and Indian wild cats (Palanisamy *et al*., 2018).

The dorsal margin of the scapula extended from the position of the proximal limb of the 1st rib to the midpoint of the 6th rib. The contour of this margin was thick and rugged, designed for scapular cartilage attachment, though this cartilage was absent at the time of sample collection. The cranial margin of scapular protuberance demonstrated as light convexity, spanning from the scapular notch (*incisura scapulae*) to the cranial angle (*angulus cranialis*) (Fig. 1a). This margin's outline was rounded and rough, yet in Indian wild cats, it appeared thinner and distinctly circular (Palanisamy *et al*., 2018).

The caudal (axillary) margin was straight with a thick and rough texture and extended from the caudal angle (*angulus caudalis*) to the glenoid depression (Fig. 1a) The cranial angle (*angulus cranialis*) did not possess distinct separation but rather fused with the adjacent margin. In contrast, the caudal angle (*angulus caudalis*) presented a robust, rugged, and tuberous-like structure. Furthermore, the ventral angle (*angulus ventralis*) of the scapula articulated with the humerus through the glenoid cavity (*cavitas glenoidalis*) of the scapula and the head of the humerus.

The glenoid cavity (cavitasglenoidalis) appeared as a round-shaped extension with a concave cavity (Fig. 1b), which exhibited variability across species. For instance, it displayed an elongated shape in elephants (Ahasan *et al*., 2016), an oval to quadrangular shape in tigers (Tomar *et al*., 2018), and an oval shape in Indian wild cats (Palanisamy *et al*., 2018). On the medial surface of the scapula, the subscapular fossa

(*fossa subscapularis*) was profoundly concave (Fig. 2a) and consists of two distinct prominent ridges: an anterior ridge and a posterior ridge. The anterior ridge, curved in nature, initiated from the lower one-third of the cranial margin and became more prominent towards the distal end. In contrast, the posterior ridge was straight, originating just below the caudal angle, running parallel to the caudal periphery, gaining prominence towards the distal end, and terminating above the rim of the glenoid cavity (*cavitas glenoidalis*). However, arelativelyshallower subscapular fossa with two crests was seen intigers (Tomar *et al*., 2018), whereas four crests were identified in civet cats (Sarma *et al*., 2017). This disparity arises from species differences. In this study, a small, nearly rounded coracoid process (processuscoracoideus) was also observed. This process was directed medially, curving backward and downward.

Table 1: Macroscopic characteristics of the Hippopotamus scapula

Parameters	**Right (Mean ± SE)**	**Left (Mean ± SE)**
Weight (g)	1960.5 ± 50.34	1910.8 ± 45.50
Maximum length (Dorsal margin to glenoid cavity) (cm)	41.88 ± 1.78	40.67 ± 1.75
Maximum width (Cranial margin to caudal angle) (cm)	29.89 ± 1.25	29.32 ± 1.24
Length of cranial margin (cm)	36.94 ± 1.62	36.21 ± 1.60
Length of caudal margin (cm)	35.56 ± 1.55	34.03 ± 1.52
Length of dorsal margin (cm)	22.08 ± 0.89	21.45 ± 0.94
Length of scapular spine (cm)	37.95 ± 1.68	35.17 ± 1.64
Height of scapular spine from supraspinous fossa (cm)	5.5.91 ± 0.33	6.75 ± 0.35
Height of scapular spine frominfraspinous fossa (cm)	7.90 ± 0.52	6.33 ± 0.50
Maximum width of supraspinous fossa (cm)	9.56 ± 0.67	8.05 ± 0.63
Maximum width ofinfraspinous fossa (cm)	11.76 ± 0.85	11.23 ± 0.82
Length of glenoid cavity (cm)	10.87 ± 0.45	10.23 ± 0.43
Width of glenoid cavity (cm)	7.70 ± 0.50	7.50 ± 0.48
Distance between glenoidcavity and acromion process (cm)	10.79 ± 0.45	10.08 ± 0.43

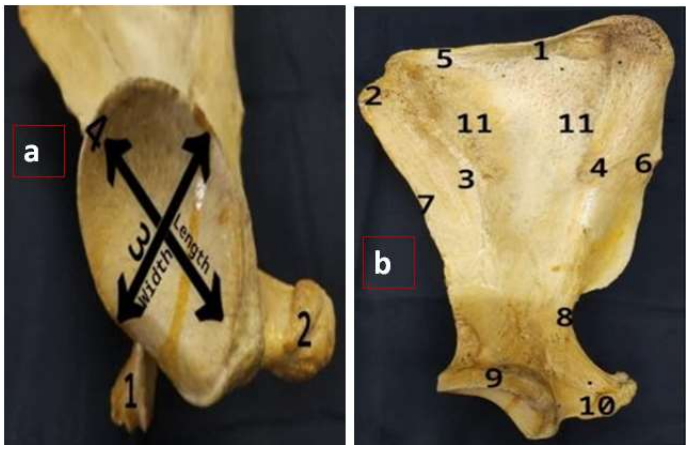

Figure 1a: Lateral view of left scapula of hippo.1= Cranial angle (*Anguluscranialis*), 2= Caudal angle (*Anguluscaudalis*), 3= Cranial margin, 4= Caudal margin, 5= Supraspinous fossa (*Fossa supraspinata*), 6= Infraspinous fossa (*Fossa infraspinata*), 7= Scapular spine (*Spina scapulae*), 8= Tuberosity of spine, 9= Suprahamate process (*Processus suprahamatus*), 10= Hamate process (*Processus hamatus*), 11= Scapular notch (*Incisura scapulae*) and 12= Coracoids process (*Processus coracoideus*). **Figure 1b:** Ventral view of left scapula of hippo. 1= Hamate process (*Processus hamatus*), 2= Suprahamate process (*Processus suprahamatus*), 3= Glenoid cavity (*Cavitasglenoidalis*) and 4= Coracoid process (*Processus coracoideus*).

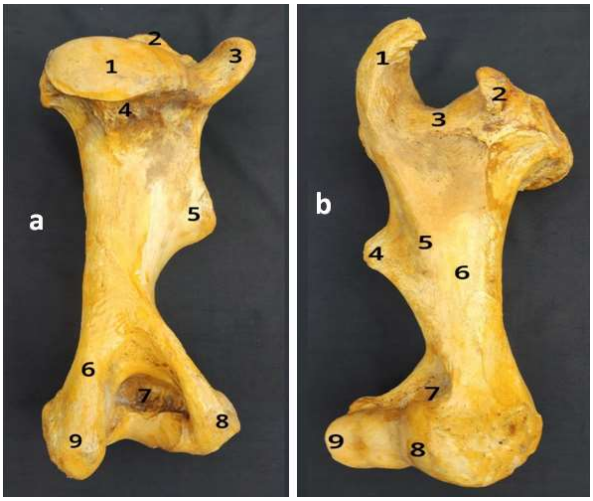

Figure 2a: Medial view of left scapula of hippopotamus. 1= Cranial angle (*Angulus cranialis*), 2= Caudal angle (*Angulus caudalis*), 3= Caudal ridge, 4= Cranial ridge, 5= Dorsal margin, 6= Cranial margin, 7= Caudal margin, 8= Scapular notch (*Incisura scapulae*), 9= Glenoid cavity (*Cavitas glenoidalis*), 10= Coracoid process (*Processus coracoideus*) and 11= Subscapular fossa (*Fossa subscapularis*). **Figure 2b**: Caudal view of right humerus of hippo. 1= Head of humerus (Caput humerus), 2= Greater or major tubercle (Tuberculum majus), 3= Lesser tubercle (*Tuberculum minus*), 4= Neck of humerus (*Collum humeri*), 5= Deltoid tuberosity (*Tuberositas deltoidea*), 6= Supracondyloid crest or ridge (*Crista supracondylaris lateralis*), 7= Olecranon fossa (*Fossa olecrani*), 8= Lateral epicondyle (*Epicondylus lateralis*) and 9= Medial epicondyle (*Epicondylus medialis*).

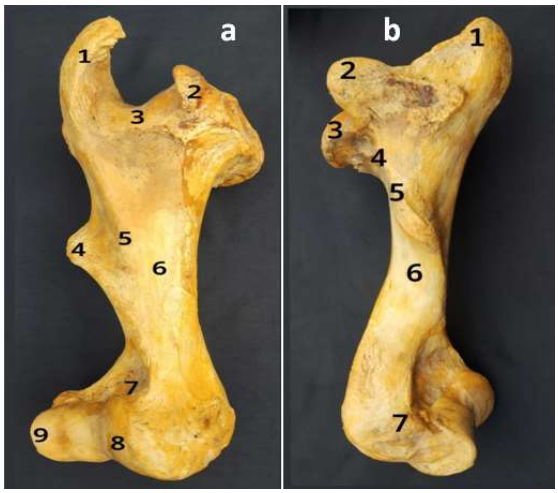

Figure 3a: Cranial view of left humerus of hippo. 1= Greater or major tubercle (*Tuberculum majus*), 2= Lesser tubercle (*Tuberculum minus*), 3= Intertubercular groove, 4= Teres major tuberosity (*Tuberositas teres majus*), 5= Deltoid tuberosity (*Tuberositasdeltoidea*), 6= Shaft of humerus (*Corpus humeri*), 7= Radial fossa (*Fossa radialis*), 8= Capitulum (*Capitulum humeri*) and 9= Trochlea (*Trochlea humeri*). **Figure 3b:** Medial view of left humerus of hippo. 1= Lesser tubercle (*Tuberculum minus*), 2= Head of humerus (*Caput humerus*), 3= Neck of humerus (*Collum humeri*), 4= Crest of lessser tubercle, 5= Shaft of humerus (*Corpus humeri*) and 6= Medial epicondyle (*Epicondylus medialis*).

Table 2: Macroscopic characteristics of the Hippopotamus humerus

Parameters	Right (Mean ± SE)	Left (Mean ± SE)
Weight (g)	2758.70 ± 70.64	2658.25 ± 66.48
Total length (cm)	46.56 ± 1.82	45.97 ± 1.80
Shaft		
Length (cm)	27.63 ± 1.32	27.24 ± 1.30
Circumference of upper part (cm)	28.90 ± 1.35	28.18 ± 1.33
Circumference of middle part (cm)	26.89 ± 1.28	26.23 ± 1.26
Circumference of lower part (cm)	29.93 ± 1.39	29.22 ± 1.37
Circumference of head (cm)	28.87 ± 1.34	28.27 ± 1.32
Proximal epiphysis		
Circumference (cm)	45.82 ± 1.80	45.43 ± 1.78
Width (cm)	22.60 ± 0.88	22.88 ± 0.89
Distal epiphysis		
Circumference (cm)	40.97 ± 1.75	40.07 ± 1.73
Width (cm)	20.67 ± 0.78	20.12 ± 0.76
Depth of olecranon fossa (cm)	7.43 ± 0.22	7.05 ± 0.21

Radius and Ulna

The radius and ulna were twin bones of the skeleton of the ante-brachium which formed the elbow joint proximally with the humerus and carpal joint distally with the carpal bones. In the hippopotamus, the articulation of the radius to the ulna occurred in a craniomedial orientation distally and craniolateral orientation proximally. Table 3 and 4 provided morphometric details for various parameters of the

hippopotamus radius and ulna. The radius has a long shaft (*corpus radii*) and two limbs, the distal limb being longer and enlarged in comparison to the proximal one. The head's proximal surface contained a concave depression known as the fovea capitis radii, which was articulated with the lateral condyle of the humerus (Fig. 4a). A rough, prominent eminence, known as the radial tuberosity (*tuberositas radii*), was situated on the medial surface of the proximal limb (Fig. 4a), as observed in tigers (Tomar *et al*., 2018).The shaft of the radius (*corpus radii*) demonstrated a slight craniocaudal expansion. Four distinct surfaces were observed: anterior, posterior, lateral, and medial. The anterior surface was rough, facilitating muscle and tendon attachment, while the posterior surface was gently convex. The lateral and medial surfaces had relatively smoother and rounded contours. The distal limb constituted the largest segment of the radius bone. An extended projection on the medial side, known as the styloid process of the radius (*processus styloideus radii*), was present (Fig. 4b). After the humerus, the ulna was the second longest bone in the hippopotamus' forelimb. Compared to the radius, at the proximal limb, the olecranon of the ulna extended further (Fig.4a), which was similar to that observed in cattle (Budras and Habel, 2011) and sheep (Sisson *et al*., 1975), but differing from the horse (Sisson *et al*., 1975). The terminal end of olecranon was caudolaterally expanded to form olecranon tuber (tuber olecrani) as observed in dogs (Sisson *et al*., 1975), and the Asiatic cheetahs (Nazem *et al*., 2017). The humeral trochlea was articulated with the large trochlear (semilunar) notch (*incisura trochlearis*) of the ulna. This articulation continued distally through the medial and lateral coronoid processes (*processus coronoideus*) to form a concave surface for joint formation. Proximally, this articulation was extended into the anconeal process (*processus anconeus*). Resembling the shape of the radius shaft, the ulna's shaft (*corpus ulnae*) took a somewhat triangular form. The proximal half of the shaft was as thick as the caudal part's distal view. At the distal limb, an extended styloid process (*processus styloideus ulnae*) was evident (Fig. 4a), which articulated with the carpal bones, as observed in the study by Nzalak *et al*., (2010). Medially, a convex facet was articulated with the radius, while cranially, the interosseous space between the radius and ulna was longer than the caudal view.

.

Table 3: Macroscopic characteristics of the Hippopotamus radius

Parameters	Right (Mean ± SE)	Left (Mean ± SE)
Total length (cm)	31.15 ± 0.79	31.27 ± 0.72
Proximal limb of radius		
Circumference (cm)	13.56 ± 1.31	13.1 ± 1.39
Width (cm)	4.01 ± 0.37	4.00 ± 0.29
Distal limb of radius		
Circumference (cm)	14.70 ± 1.45	14.15 ± 1.43
Width (cm)	4.85 ± 0.40	4.60 ± 0.38
Circumference at mid shaft (cm)	1.32 ± 0.2	1.20 ± 0.1

Table 4: Macroscopic characteristics of the Hippopotamus ulna

Parameters	Right (Mean ± SE)	Left (Mean ± SE)
Total length (cm)	40.86 ± 1.03	41.18 ± 0.88
Circumference		
Proximal limb (cm)	13.92 ± 1.41	13.80 ± 1.35
Distal limb (cm)	12.68 ± 1.35	12.42 ± 1.33
Length of olecranon (cm)	10.68 ± 1.25	10.15 ± 1.20
Circumference at distal limb of olecranon (cm)	11.80 ± 1.28	11.25 ± 1.26

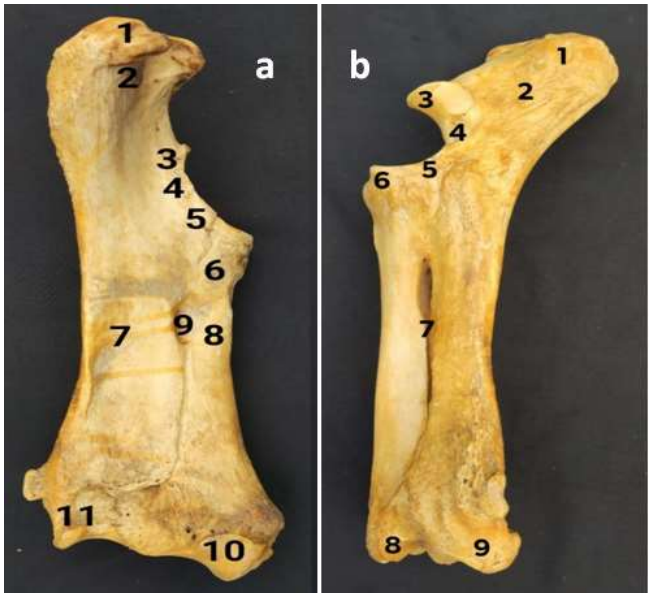

Figure 4a: Caudomedial view of right radius and ulna of hippo. 1= Olecranon tuber (*Tuber olecrani*), 2= Olecranon process (*Processus olecrani*), 3= Anconeal process (*Processus anconeus*), 4= Trochlear notch (*Incisura trochlearis*), 5= Capitular fovea of radius, 6= Radial tuberosity (*Tuberositas radii*), 7= Shaft of ulna (*Corpus ulnae*), 8= Shaft of radius (*Corpus radii*), 9= Interosseous space, 10=Styloid process of ulna (*Processus styloieus ulnae*) and 11=Styloid process of radius (*Processus styloieus radii*). **Figure 4b:** Craniomedial view of right radius and ulna of hippo. 1= Olecranon tuber (*Tuber olecrani*), 2= Olecranon process (*Processusolecrani*), 3= Anconeal process (*Processus anconeus*), 4= Trochlear notch (*Incisura trochlearis*), 5= Coronoid process (*Processus coronoideus*), 6= Capitular fovea of radius, 7= Interosseous space, 8= Styloid process of radius (*Processus styloieus radii*) and 9= Styloid process of ulna (*Processus styloieus ulnae*).

Conclusion

The detailed examination of hippopotamus forelimb bones, including their unique anatomical traits and precise morphometric measurements, holds practical significance. These insights are pertinent for identification, radiographic interpretation, and forensic investigations involving these bones. The comprehensive information provided serves as a concise and informative guide for understanding the distinct anatomical parameters of hippopotamus forelimb bones.

Acknowledgement

The authors would like to thank Rangpur Recreation Park and Zoo for the providing of dead body of Hippopotamus and department of livestock services for proper administrative support. We also sincerely acknowledge the financial cooperation of Patuakhali Science and Technology University.

Conflict of interest

Authors declare no conflicts of interest

References

1. Ahasan ASM, Quasem M, Rahman ML, Hasan RB, Kibria ASM and Shil SK. Macroanatomy of the bones of thoracic limb of an Asian elephant (Elephas maximus). International Journal of Morphology. 2016; 34(3): 909-917.
2. Brittany C and Frank F. Hippopotamus Underwater Locomotion: Reduced-Gravity Movements for a Massive Mammal. 2009.
3. Budras KD and Habel RE. Bovine Anatomy: An Illustrated Text. Hannover, Schlütersche. 2011.
4. Eltringham SK. The hippos: natural history and conservation. T&A D Poyer, London, United Kingdom. 1999.
5. Feldhamer GA, Drickamer LC, Vessey SH and Merritt JF. Mammalogy. McGraw-Hill, Boston, Massachusetts.1999.
6. Fisher RE, Scott KM and Naples VL. Forelimbmyology of the pygmy hippopotamus (Choeropsisliberiensis). Anatomical Record. 2007; 290: 673–693.
7. Klingel H. Sizing up a heavyweight. International Wildlife. 1991; 21: 4–11.
8. Miller CE, Basu C, Fritsch G, Hildebrandt T and Hutchinson JR. Ontogenetic scaling of foot musculoskeletal anatomy in elephants. J. R. Soc. Interface. 2008; 5(21): 465-475.
9. Nazem MN, Sajjadian SM and Nakhaei A. Anatomy, functional anatomy and morphometrical study of forelimb column in Asiatic cheetah (*Acinonyx jubatus venaticus*). Italian Journal of Anatomy and Embryology. 2017; 122 (3): 157-172.
10. Nowak RM. Walker's mammals of the world. 6th ed. JohnsHopkins University Press, Baltimore, Maryland. 1999.
11. Nzalak JO, Eki MM, Sulaiman MH, Umosen AD, Salami SO, Maidawa SM and Ibe CS. Gross anatomical studies of the bones of the thoracic limbs of the Lion (Panthera leo). Journal of Veterinary Anatomy. 2010; 3(2): 65-71.
12. Palanisamy D, Tomar MPS, Ankem PB, Ullakula RS, Jonnalagadda N and Korampalli V. Gross morphology of scapula in Indian wild cat (Felis silvestris ornate: Gray, 1830). International Journal of Current Microbiology and Applied Sciences. 2018; 7(4): 2473-2477.
13. Sarma K, Sasan JS and Suri S. Gross and morphometrical studies on scaputhe la of civet cat (Viverricula indica). International Journal of Pure and Applied Bioscience. 2017; 5(6): 80-85.
14. Sisson S, Grossman JD and Getty R. Sisson and Grossman's The Anatomy of the Domestic Animals. 5th ed. Philadelphia, W. B. Saunders Press. 1975.
15. Tomar MPS, Taluja JS, Vaish R, Shrivastav AB, Shahi A and Sumbria D. Gross anatomy of scapula in tiger (Panthera tigris). Indian Journal Animal Research. 2018; 52(4): 547-550.
16. Wall WP. The correlation between high limb-bone density and aquatic habits in Recent mammals. Journal of Paleontology. 1983; 57:197–207.